

Curing Behavior and Viscoelasticity of Dual-Curable Adhesives Based on High-Reactivity Azo Initiator

JONG-GYU LEE,^{1,5} GYU-SEONG SHIM,^{1,6} JI-WON PARK,^{1,2,7}
HYUN-JOONG KIM,^{1,2,8} SANG-EUN MOON,^{3,9} YOUNG-KWAN KIM,^{3,10}
DONG-HUN NO,^{3,11} JONG-HWAN KIM,^{3,12} and KWAN-YOUNG HAN^{3,4,13}

1.—Laboratory of Adhesion and Bio-Composites, Program in Environmental Materials Science, Seoul National University, Seoul 151-921, Republic of Korea. 2.—Research Institute of Agriculture and Life Sciences, Seoul National University, Seoul 151-921, Republic of Korea. 3.—Samsung Display, Asan 336-140, Republic of Korea. 4.—Display Engineering, College of Convergence Technology, Dankook University, Cheonan 330-714, Republic of Korea. 5.—e-mail: spdh123@snu.ac.kr. 6.—e-mail: sks6567@snu.ac.kr. 7.—e-mail: roorouny@gmail.com. 8.—e-mail: hjokim@snu.ac.kr. 9.—e-mail: se.moon@samsung.com. 10.—e-mail: ykwan13.kim@samsung.com. 11.—e-mail: donghun.no@samsung.com. 12.—e-mail: jh0511.kim@samsung.com. 13.—e-mail: jungwu619@naver.com

We have investigated the curing behavior of dual-curable acrylic resin to solve problems associated with curing of adhesives in shaded areas during display manufacture. A low-temperature curing-type thermal initiator, 2,2'-azobis (4-methoxy-2,4-dimethylvaleronitrile), with a 30°C half-life decomposition temperature was used in the investigation. Dual-curable adhesives were prepared according to the thermal initiator content and ultraviolet (UV) radiation dose. The effects of thermal initiator and UV irradiation on the curing behavior and viscoelasticity were investigated. Using Fourier-transform infrared spectroscopy and gel-fraction analysis, an evaluation was carried out to determine the degree of curing after dual UV/thermal curing. In addition, the real-time curing behavior was evaluated using thermogravimetric analysis, differential scanning calorimetry, and a UV/advanced rheometric expansion system. A lift-off test was carried out to verify the effects of dual curing on adhesion performance. Application of UV irradiation before thermal curing suppressed the thermal curing efficiency. Also, the network structure formed after dual curing with low UV dose showed higher crosslinking density. Therefore, the thermal initiator radical effectively influenced uncured areas with low curing temperature and initiator content without causing problems in UV-curable zones.

Key words: Dual-curable adhesive, dual-curing behavior, optically clear resin, rheology

INTRODUCTION

Because ultraviolet (UV) curing has distinct advantages, it is widely used in various industries such as ink printing, surface coating, and adhesive manufacture. The recent increased use and expansion of this technology are due to its advantage of rapid curing rate.¹ In addition, UV curing is a

solvent-free process, can be performed at ambient temperature, and has high polymerization rate.² UV radical polymerization has mainly been studied, because radical curing is achieved at a faster rate than in other curing methods such as ionic polymerization, step polymerization, or vaporization. Acrylate-based resin is especially used in UV radical polymerization because of its high monomer reactivity.^{3,4} However, the UV curing process has a number of limitations; For example, curing is prevented in shaded areas, such as on curved

(Received November 16, 2015; accepted March 24, 2016; published online April 11, 2016)

surfaces, because it is not possible for light to reach such surfaces.⁵ This has implications for the reliability of UV curing, because any remaining, unreacted monomer will act as a defect in the product. Such monomers can contaminate other parts of the product, such as the cover glass of a display. For these reasons, UV curing treatment alone is insufficient for display bonding processes.

The transparent adhesive resin used for display bonding is called optically clear resin (OCR). The

applications of optical bonding adhesives include not only simple bonding of touchscreen panels (TSPs), but also improvement of display image quality by filling air gaps, while also protecting the TSP from external damage.⁶ Adhesive materials for optical applications demand high transparency for improvement of quality, nonacidic conditions for prevention of TSP corrosion, appropriate viscoelastic properties for damping damage, and low shrinkage. The display bonding process between the TSP and cover glass is a UV curing process using OCR.⁷ The TSP and cover glass are temporarily fixed by precuring to prevent overflow, and the display is then completely cured in the final curing process. However, under shaded areas, monomers cannot be cured due to obstruction by the black matrix (BM) area. Although side-curing treatment is undertaken during or after the final curing process, this is not sufficient to cure the monomers under the BM area due to the flexible printed circuit board (FPCB), which interferes with the UV light path. Therefore, other curing methods undisturbed by obstacles are required for curing in such shaded areas. We applied and investigated a dual UV/thermal curing process, as shown in Fig. 1. A thermal initiator for curing at ambient temperature is required, because the TSP could be damaged by heating at temperatures above 100°C, and short process time is required. In this process, both the thermal curing behavior and mechanical properties are affected by the degree of UV precuring caused by penetration of UV light.⁸ To solve the curing problems related to UV curing, dual-curing systems such as a redox system, isocyanate linkage, and urethane linkage have been investigated,^{9,10} however, it is difficult to apply these methods for the current process because of the demand for additional processing steps.

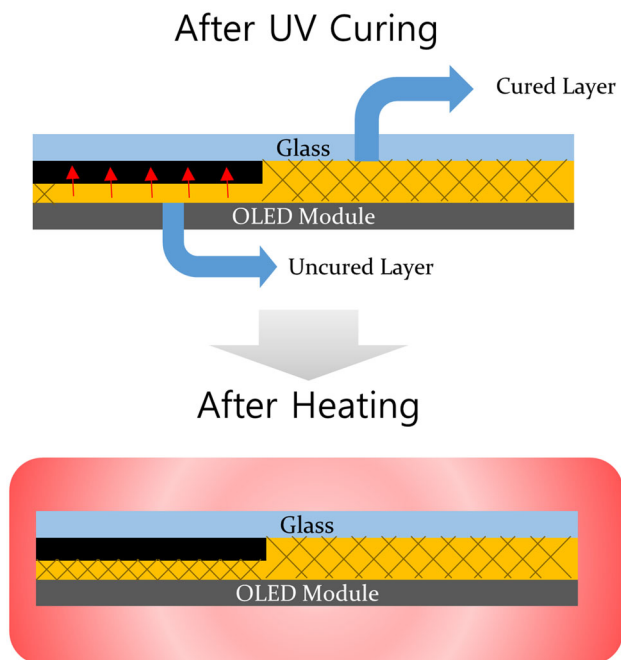


Fig. 1. Schematic diagram of dual-curing process.

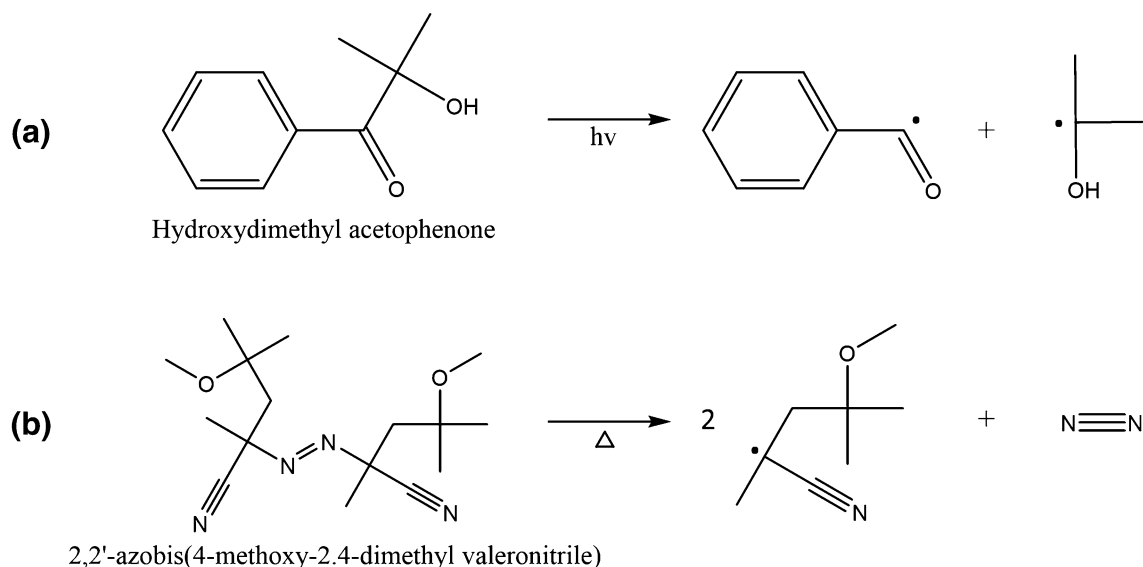


Fig. 2. Free-radical generation of (a) photoinitiator and (b) thermal initiator.

Table I. Raw materials for synthesis and preparation of optically clear resin

| Function | Material | Abbreviation | Molecular weight (g/mol) | Glass-transition temperature (°C) | Content (wt.%) | Supplier |
|--------------------|--|--------------|--------------------------|-----------------------------------|----------------|--------------------------|
| Acrylic monomer | 2-Ethylhexyl acrylate | 2-EHA | 184.28 | -70 | 61 | Sigma Aldrich |
| Acrylic monomer | Isobornyl acrylate | IBA | 208.3 | 94 | 35 | Sigma Aldrich |
| Functional monomer | <i>N</i> -vinyl caprolactam | VC | 139.19 | 184 | 4 | Tokyo Chemical Industry |
| Crosslinking agent | Poly(ethylene glycol) 200 dimethacrylate | PEGDMA200 | 330.4 | — | 1 phr | Miwon Specialty Chemical |

In this study, 2,2'-azobis(4-methoxy-2,4-dimethylvaleronitrile), with 10-h half-life decomposition temperature of 30°C, was used as thermal initiator for dual UV/thermal curing, as shown in Fig. 2. However, this initiator is unstable at excessive initiator content, because azo-based initiators cause bubbles and yellowing.¹¹ For this reason, the thermal curing efficiency cannot be improved by adding excess initiator. Acrylate resin was made with 2-ethylhexyl acrylate, isobornyl acrylate, and *N*-vinyl caprolactam. *N*-vinyl caprolactam was used as a nonacidic monomer instead of acrylic acid to control the glass-transition temperature and improve the cohesion properties. Resin was used in the form of prepolymer composed of oligomer and monomer without solvent for viscosity adjustment. The curing kinetics of the dual-curable acrylate resin was measured for various initiator contents and degrees of prior UV irradiation. The dual-curing behavior was analyzed by Fourier-transform infrared (FR-IR) spectroscopy, differential scanning calorimetry (DSC), a UV/advanced rheological expansion system (UV-ARES), and gel-fraction analysis. In addition, changes in the mechanical properties were determined by lift-off testing. The thermal degradation and curing behavior under heating conditions was evaluated by thermogravimetric analysis.

EXPERIMENTAL PROCEDURES

Materials

2-Ethylhexyl acrylate (Sigma Aldrich, USA), isobornyl acrylate (Sigma Aldrich, USA), and *N*-vinyl caprolactam (Tokyo Chemical Industry, Japan) were used as monomers without purification. Poly(ethylene glycol) 200 dimethacrylate (Miwon Specialty Chemical, Republic of Korea) was used as crosslinking agent, as shown in Table I. Hydroxydimethyl acetophenone (Miwon Specialty Chemical, Republic of Korea) was used as photoinitiator. 2,2'-Azobis(4-methoxy-2,4-dimethylvaleronitrile) (Wako Pure Chemical Industries, Japan) was used as thermal initiator.

Characterization Methods

Prepolymer Synthesis

Adhesives were synthesized using 2-ethylhexyl acrylate, isobornyl acrylate, and *N*-vinyl caprolactam via bulk radical polymerization. Mixtures of monomers were initiated with 1 wt.% hydroxydimethyl acetophenone. Polymerization was performed in a 500-mL four-necked round-bottomed flask equipped with mechanical stirrer, N₂ inlet, thermometer, and light-emitting diode (LED) UV lamp. The temperature was maintained at room temperature with constant stirring at 100 rpm. After N₂ purging for 30 min under constant stirring, the monomer mixtures were subsequently exposed to a UV lamp (20 mW/cm²) for 70 s at room temperature under N₂ purging.¹²

Adhesive Film Preparation

UV-curable adhesive syrups were prepared by blending of prepolymer with crosslinking agent [poly(ethylene glycol) 200 dimethacrylate, 1 phr] and thermal initiator. The mixture was blended by a paste mixer with a revolution at 600 rpm, and rotation at 500 rpm for 3 min. Syrup was coated at thickness of 45 μm on corona-treated polyethylene terephthalate films (PET, SKC Co. LTD., Republic of Korea). The coated resin was cured by passing under a conveyor-type UV-curing machine equipped with medium-pressure mercury UV lamps (154 mW/cm², main wavelength 365 nm). The UV irradiation doses were 200 mJ/cm², 400 mJ/cm², 600 mJ/cm², 800 mJ/cm², 1600 mJ/cm², and 2500 mJ/cm², as measured using a UV radiometer (IL 390C Light Bug, International Light Inc.). Each adhesive, with various degrees of curing, was cured in an oven at 80°C for 60 min.

Fourier-Transform Infrared (FT-IR) Spectroscopy

Infrared reflectance spectra were measured using an FT-IR spectrometer (JASCO FTIR-6100) with Mylar beam splitter. Spectra were collected for 32 scans at resolution of 4 cm⁻¹ between 400 cm⁻¹ and 4000 cm⁻¹. Acrylate double-bond conversion after given irradiation time (t) was calculated using Eq. 1:

$$\text{Conversion}(\%) = \frac{(A_{810})_0 / (A_{1720})_0 - (A_{810})_t / (A_{1720})_t}{(A_{810})_0 / (A_{1720})_0} \times 100, \quad (1)$$

where $(A_{810})_0$ is the initial intensity at 810 cm⁻¹, $(A_{810})_t$ is the intensity at 810 cm⁻¹ at time t , $(A_{1720})_0$ is the initial intensity at 1720 cm⁻¹, and $(A_{1720})_t$ is the intensity at 1720 cm⁻¹ at time t .

Gel Fraction

The gel fraction of the dual-cured adhesives was determined by soaking samples of 0.2 g to 0.3 g in toluene for 1 day at room temperature. The insoluble part of the adhesive was then removed by filtration

and dried at 70°C to constant weight, as shown in Fig. 3. The gel fraction was calculated by Eq. 2:

$$\text{Gel fraction}(\%) = \frac{W_1}{W_0} \times 100, \quad (2)$$

where W_0 is the weight before filtration and W_1 is the weight after filtration.

Thermogravimetric Analysis (TGA)

TGA measurements were carried out using a thermogravimetric analyzer (TGA 4000, PerkinElmer, USA). Samples of 4 mg to 5 mg were evaluated from 30°C to 400°C at heating rate of 5°C/min. During testing, the green composites were placed in a high-quality nitrogen atmosphere (99.5% nitrogen, 0.5% oxygen content) to prevent unwanted oxidation.

Differential Scanning Calorimetry (DSC)

DSC measurements were carried out on samples of 7 mg to 8 mg using a TA Q200 device in the temperature range from -50°C to 200°C at scan rate of 5°C/min, and during cooling at the same rate, in dynamic mode under nitrogen atmosphere. The thermal curing behavior was determined from the first scan, and the glass-transition temperature (T_g) was determined from the second scan.

UV/Advanced Rheometric Expansion System (UV-ARES) Analysis

The viscoelastic properties of the acrylic adhesives were determined using an advanced rheometric expansion system (ARES, Rheometric Scientific, UK) with 8-mm parallel-plate geometry. The typical temperature scan range was from -30 °C to 150°C at heating rate of 2°C/min, while the cooling rate was 10°C/min. The frequency was 1 Hz, and the gap between the plates was 1 mm. In addition, $\tan \delta$ - curves from the temperature sweep tests suggested the T_g value at the second cycle. UV light irradiation was performed using a medium-pressure mercury lamp with intensity of 200 mW/cm² for 5 s to 15 s.

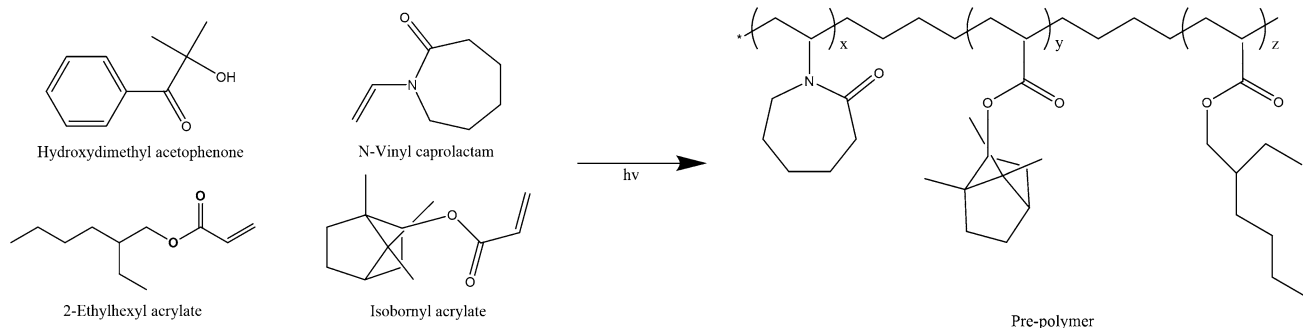


Fig. 3. Synthesis of acrylic prepolymer.

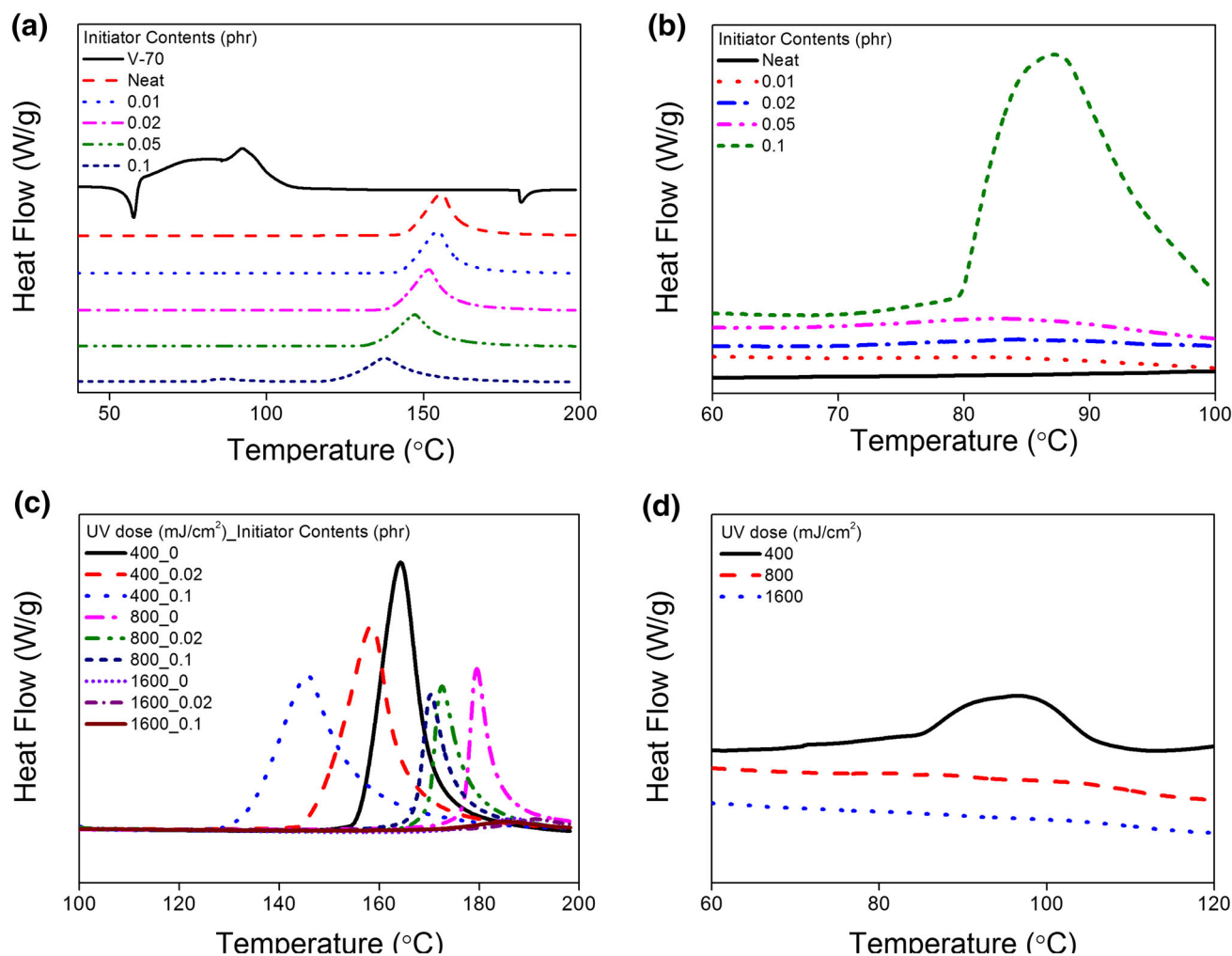


Fig. 4. Thermal curing behavior of acrylic resin with different initiator contents (a) without UV dose and (c) with UV doses of 400 mJ/cm², 800 mJ/cm², and 1600 mJ/cm². Exothermic peaks of reaction of thermal initiator (b) without UV dose and (d) with UV doses of 400 mJ/cm², 800 mJ/cm², and 1600 mJ/cm² containing 0.1 phr initiator.

RESULTS AND DISCUSSION

Curing Behavior of Acrylic Resin Determined by DSC and TGA

DSC experiments were carried out to measure the thermal curing behavior of precured acrylic resin. Although the thermal initiator had a 10-h half-life decomposition temperature of 30°C, the specific temperature should be adjusted for application in manufacture to reduce the process time. The C=C double bond is broken by radical polymerization as the temperature of the acrylic resin increases and the thermal initiator reacts.¹³ The exothermic reaction caused by polymerization was compared with the reaction of the thermal initiator. In the DSC curves, two types of exothermic peak were observed: one between 70°C and 100°C, and the other between 120°C and 200°C. The first peak indicates the thermal curing reaction, while the second peak shows the reaction of acrylate monomer.

The change of the second exothermic peak indicates that the reaction of monomers was accelerated

by increase in the initiator content, as shown in Fig. 4a. In addition, the second exothermic peak shifted to lower temperature and decreased in height as the initiator content was increased. Figure 4b shows that the first exothermic peak increased with increase of the thermal initiator content from 0.01 phr to 0.1 phr. The exothermic peak was barely visible for low initiator contents under 0.1 phr, but the peak height for the resin containing 0.1 phr initiator increased rapidly. The DSC results in Fig. 4c also show that the height of the peak and the shift tendency decreased as the initiator content was increased. Otherwise, the exothermic peak decreased with a shift to higher temperature due to suppression of thermal curing, depending on the prior UV curing. Figure 4d shows the height of the second exothermic peak, indicating that the reaction of the thermal initiator with monomers decreased with increase of the UV dose, because the initial UV curing suppressed thermal curing. As the UV curing progressed, the mobility of

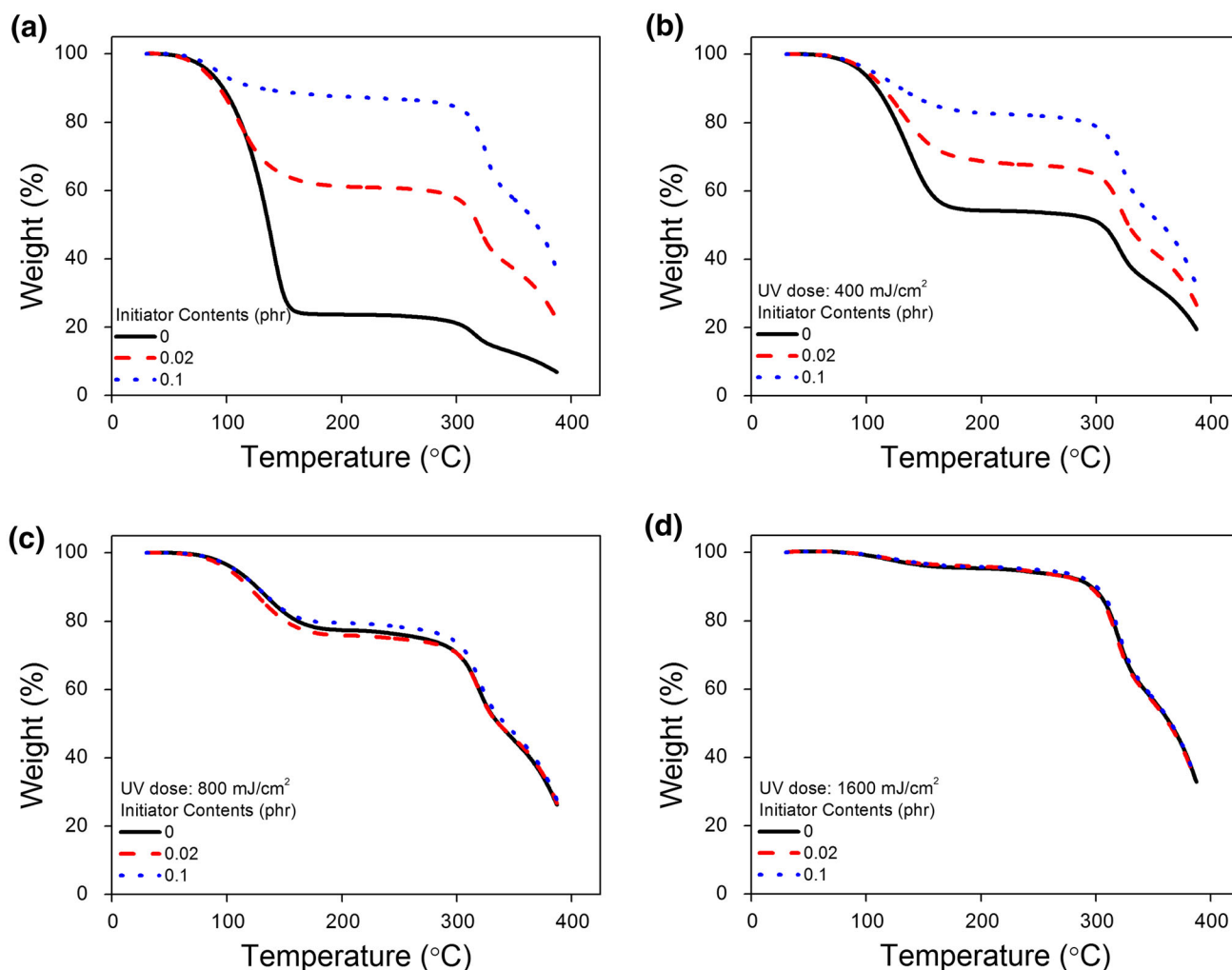


Fig. 5. Thermogravimetric analysis for different initiator contents: (a) without UV dose, and with UV doses of (b) 400 mJ/cm², (c) 800 mJ/cm², and (d) 1600 mJ/cm².

the polymer decreased because of polymer growth and network structure formation.

TGA measured the weight loss, revealing the ratio of polymers and indicating the degree of thermal curing. The results for the thermal curing behavior of the acrylic resin are shown in Fig. 5. Decomposition progressed in two steps; the first step showed volatilization of unreacted monomer and moisture in the adhesive film, while the second step showed polymer degradation. Figure 5a shows the weight loss of resin not irradiated with UV light from 30°C to 400°C. The temperature at which the plateau occurred shifted from 170°C to 90°C as the amount of initiator was increased. In addition, the weight loss decreased from 72.6% to 5.3% in the plateau area. The weight loss of 72.6% for neat resin was caused by prepolymer degradation. In Fig. 5b, the adhesives with 400 mJ/cm² UV dose also showed a change as the weight loss gap decreased. In contrast, Fig. 5c and d shows the weight loss of adhesives with various initiator contents and UV doses. In particular, the film containing 0.1 phr

initiator without UV treatment showed greater weight loss than that exposed to 800 mJ/cm², because thermal curing was suppressed by the prior UV curing. The change in weight loss decreased as the prior UV irradiation dose was increased. At UV doses of 800 mJ/cm² and 1600 mJ/cm², thermal curing did not affect the weight loss. Also, for the UV dose of 800 mJ/cm², the weight loss showed a gel fraction of less than 80%, due to the restrained thermal curing. Therefore, the TGA results indicate that the UV dose suppressed thermal curing because the radical was caged by the decreased mobility of the polymer.

FT-IR Conversion

FT-IR spectra were obtained to analyze the number of C=C double bonds in the acrylic resin. C=C double bonds are broken as polymerization proceeds, and this chemical reaction can be confirmed by investigating the height of the peak at 810 cm⁻¹.^{14,15} Figure 6 shows the change of

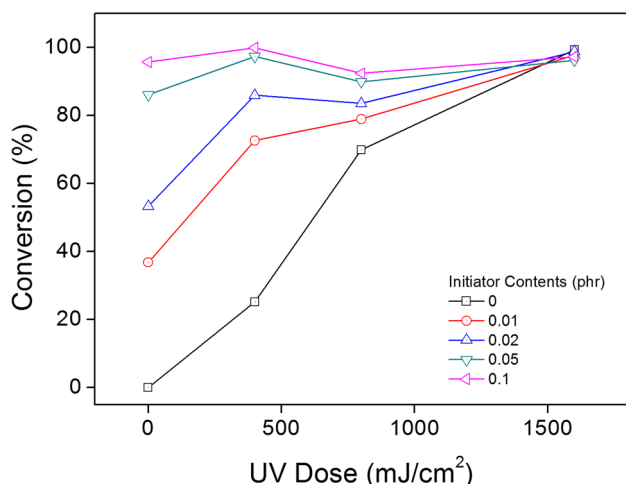


Fig. 6. FT-IR conversion at 810 cm^{-1} after dual curing as a function of UV dose and initiator content.

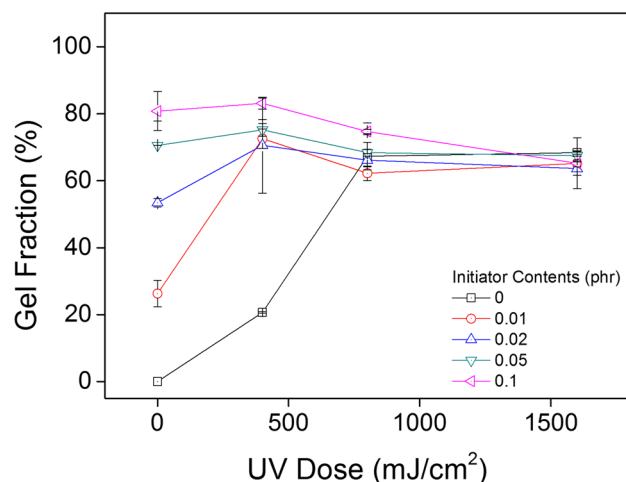


Fig. 7. Gel fraction after dual curing as function of UV dose and initiator content.

conversion according to the amount of initiator and UV dose. The conversion increased as the UV dose and thermal initiator concentration were increased. Acrylic adhesive containing less than 0.02 phr thermal initiator without UV irradiation could not be cured completely due to lack of radicals. Because 2,2'-azobis(4-methoxy-2,4-dimethylvaleronitrile) has high reactivity, it cannot be used above 0.1 phr due to insolubility, yellowing, and bubbling. The FT-IR results show that less than 0.1 phr thermal initiator could cure all of the monomers. Although the initial conversion increased with increase of the UV dose, the adhesives were not fully cured because the thermal curing efficiency was decreased by the prior UV curing. With UV dose of 400 mJ/cm^2 , the conversion increased with addition of thermal initiator. However, the conversion at 800 mJ/cm^2 was lower than at 400 mJ/cm^2 , because the thermal curing was suppressed as UV curing proceeded.

Gel Fraction

The gel fraction was measured to investigate the crosslinking of the dual-curable resin. Figure 7 shows that the change of the gel fraction was dependent on the thermal initiator content and UV dose. The gel fraction increased with increasing initiator content because the amount of monomer per initiator was limited. In addition, the gel fraction increased with decreasing UV dose due to network structure formation. Thermal curing after UV irradiation improved the network structure formation, although UV curing could not affect the crosslinking structure above a dose of 800 mJ/cm^2 . Notably, for UV dose of 400 mJ/cm^2 , network formation was accelerated. Also, extensive network structure formation occurred even for low concentration of thermal initiator. The gel fraction results show that improvement of the thermal curing efficiency improved the formation of crosslinking.

Curing Behavior and Rheological Properties Determined by UV-ARES

UV-ARES was used to examine the dual UV/thermal curing behavior for various UV doses by dynamic temperature sweeping. The rheological properties of dual-curable resin can provide quantitative data for protecting the TSP and for display and adhesion performance.¹⁶ The UV curing behavior, thermal curing behavior, and rheological properties were measured for the same sample by controlling the curing steps. Figure 8a–c shows the UV curing behavior of resin according to the thermal initiator content. The storage modulus after UV curing did not change with the initiator content. These results indicate that addition of thermal initiator did not influence the UV curing behavior or storage modulus. Figure 8d–f shows the results of ramp tests from 30°C to 150°C for measurement of the thermal curing behavior depending on the initiator content and prior UV irradiation. As the thermal initiator content was increased, the storage modulus increased because of the reaction of the thermal initiator. In addition, this increase of the storage modulus was constrained by prior UV curing, because polymerization decreased the mobility of the polymer chains. With UV doses of 800 mJ/cm^2 and 1600 mJ/cm^2 , thermal curing could not improve the storage modulus. Also, the reaction temperature for thermal initiation was accelerated with increasing thermal initiator concentration.

The viscoelastic properties of the dual-curable acrylic adhesives are shown in Fig. 8g–i. The storage modulus in the plateau area was higher than for adhesive subjected to low UV dose due to the formation of crosslinking. Also, the storage modulus at room temperature showed similar values in adhesives with 0.1 phr thermal initiator. The UV-ARES results provide information for application of this process. The thermal initiator

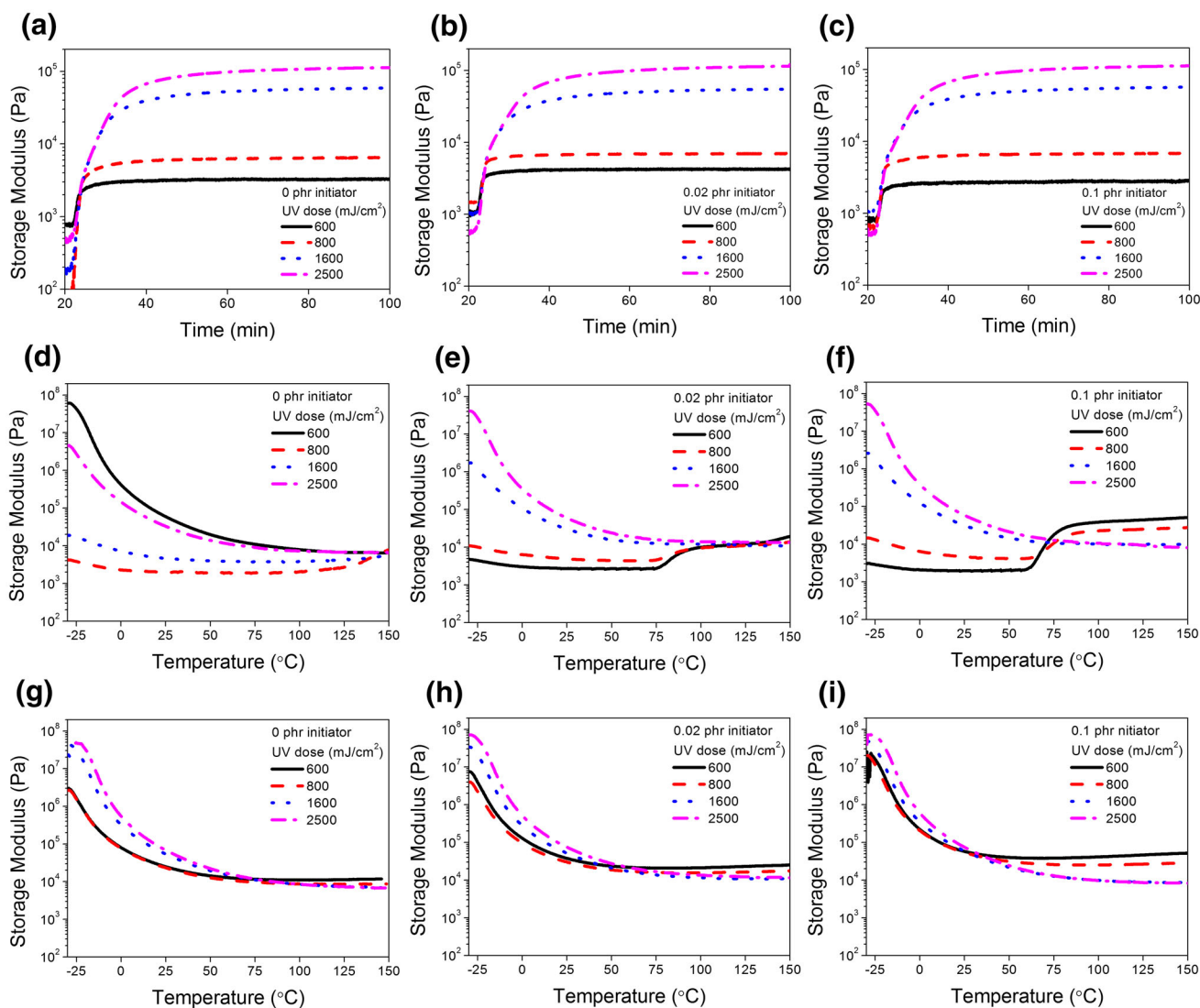


Fig. 8. Storage modulus of dual-curable resin as function of initiator content: (a) 0 phr, (b) 0.02 phr, and (c) 0.1 phr with UV curing; (d) 0 phr, (e) 0.02 phr, and (f) 0.1 phr for thermal curing; (g) 0 phr, (h) 0.02 phr, and (i) 0.1 phr after dual curing for measurement of rheological properties.

rarely affected the viscoelastic properties of the UV-curable zone, while resulting in proper curing behavior within the shaded area. Figure 9 shows the glass-transition temperature with increase of the UV dose and thermal initiator concentration. When the UV dose was increased, the adhesive had higher T_g because of the increase in the molecular weight of the polymer. However, T_g showed a higher value at 600 mJ/cm² than 800 mJ/cm² for the dual-cured adhesives because of greater crosslinking formation.

Results explaining the effect of dual curing on the formation of crosslinking are shown in Fig. 10. The gel fraction per conversion was calculated as $\Delta \text{gel fraction} / \Delta \text{conversion} \times \text{remaining monomers}$. The average molecular weight between crosslinks, M_c , was derived from Eq. 3, based on rubbery elasticity.¹⁷ However, the crosslinking density was

higher in film exposed to low UV dose because an interpenetrating polymer network (IPN) formed at lower thermal initiator content.

$$G_N^0 = \frac{\rho RT}{M_c}, \quad (3)$$

where G_N is the storage modulus, ρ is the density, R is the gas constant, T is the absolute temperature, and M_c is the average molecular weight between crosslinks. M_c was calculated using Eq. 3. This result shows that the network structure formed by thermal curing for low UV dose had higher crosslinking density. Such a network structure with higher crosslinking density results in decreased mobility of polymer chains, increasing the T_g value of the dual-cured adhesives.

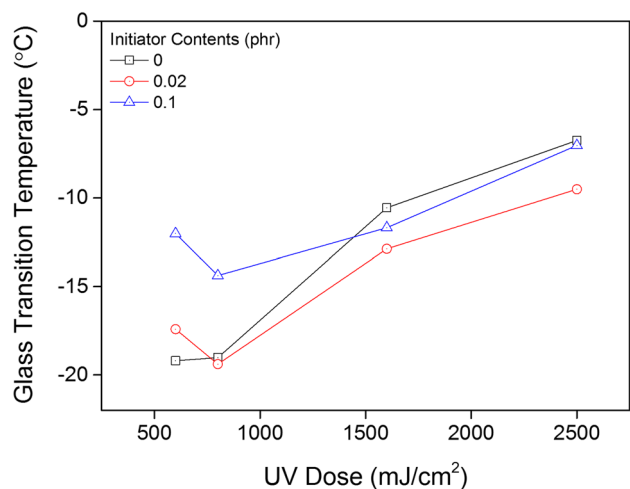


Fig. 9. Glass-transition temperature of acrylic adhesives measured by UV-ARES after dual curing.

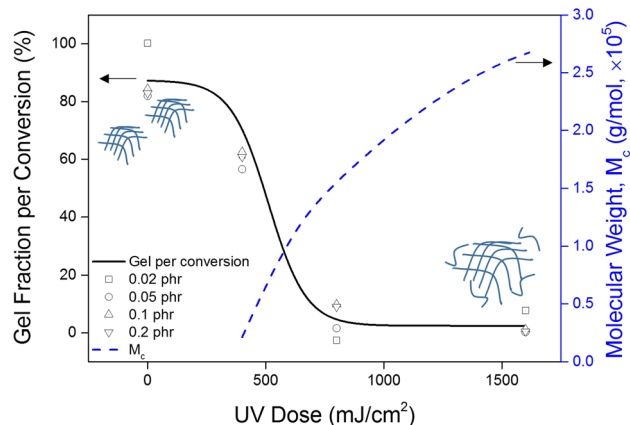


Fig. 10. Effect of UV dose on (a) crosslinking formation and (b) average molecular weight between crosslinks.

CONCLUSIONS

We demonstrate the curing behavior and viscoelasticity of dual-curable adhesives based on a radical initiation system. The curing behavior of dual-curable adhesive prepared with 2,2'-azobis(4-methoxy-2,4-dimethylvaleronitrile) was investigated. Addition of the thermal initiator improved the conversion and viscoelasticity with low concentration and reaction temperature but did not affect the UV curing behavior. As the thermal initiator

content was increased, the thermal curing efficiency increased, as shown by DSC and TGA observations. Also, thermal curing was suppressed as the UV dose was increased. However, at low UV dose, thermal initiation was accelerated. FT-IR results showed that thermal initiator concentration below 0.1 phr provided thermal curing capability for the dual-curable adhesive. Also, network structure formation was increased by thermal curing with low UV dose. The glass-transition temperature affected the curing behavior, showing minimum values at UV dose of 800 mJ/cm², due to network structure formation at lower UV doses and higher molecular weight compared with higher UV doses. The room-temperature storage modulus increased with increasing initiator content. In addition, the storage modulus in the plateau area increased only for low UV dose due to suppression of thermal curing by prior UV curing. ARES results indicated that the network structure formed in the shaded area after dual curing had higher crosslinking density.

REFERENCES

1. R.S. Davidson, *Exploring the Science, Technology and Applications of UV and EB Curing* (London: SITA Technology, 1999).
2. C. Decker, T. Nguyen Thi Viet, D. Decker, and E. Weber-Koehl, *Polymer* 42, 5531 (2001).
3. J.D. Cho and J.W. Hong, *Eur. Polym. J.* 41, 367 (2005).
4. E. Andrzejewska, *Prog. Polym. Sci.* 26, 605 (2001).
5. U. Schmidt, in *RadTech Europe Conference Proceeding* (2001), p. 53.
6. S.W. Lee, J.W. Park, Y.E. Kwon, S. Kim, H.J. Kim, E.A. Kim, H.S. Woo, and J. Swiderska, *Int. J. Adhes. Adhes.* 38, 5 (2012).
7. D. Lu, J. Wang, C. Li, and J. Yuan, in *Electronic Packaging Technology and High Density Packaging (ICEPT-HDP), 2012 13th International Conference on* (IEEE, Guilin, 2012), pp. 438–441.
8. J.W. Hwang, K.N. Kim, G.S. Lee, J.H. Nam, S.M. Noh, and H.W. Jung, *Prog. Org. Coat.* 76, 1666 (2013).
9. K. Studer, C. Decker, E. Beck, and R. Schwalm, *Eur. Polym. J.* 41, 157 (2005).
10. C. Decker, *Macromol. Mater. Eng.* 288, 17 (2003).
11. K. Studer, P.T. Nguyen, C. Decker, E. Beck, and R. Schwalm, *Prog. Org. Coat.* 54, 230 (2005).
12. S.Y. Kim, S.W. Lee, D.H. Lim, J.W. Park, C.H. Park, and H.J. Kim, *J. Adhes. Sci. Technol.* 27, 2177 (2013).
13. R.B. Prime and E.A. Turi, *Thermal Characterization of Polymeric Materials* (New York: Academic, 1981), p. 532.
14. B.S. Chiou and S.A. Khan, *Macromolecules* 30, 7322 (1997).
15. C.Y. Bai, X.Y. Zhang, J.B. Dai, and W.H. Li, *Prog. Org. Coat.* 55, 291 (2006).
16. E.P. Chang and D. Holguin, *J. Adhes.* 81, 495 (2005).
17. K. Cho, *Polymer* 37, 813 (1996).

Reproduced with permission of the copyright owner. Further reproduction prohibited without permission.